

## MODELING HEAVY ION IONIZATION LOSS IN THE MARS15 CODE

**I.L. Rakhno\*, N.V. Mokhov, and S.I. Striganov**

Fermi National Accelerator Laboratory  
MS 220, Batavia, Illinois 60510-0500  
rakhno@fnal.gov; mokhov@fnal.gov; strigano@fnal.gov

### ABSTRACT

The needs of various accelerator and space projects stimulated recent developments to the MARS Monte Carlo code. One of the essential parts of those is heavy ion ionization energy loss. This paper describes an implementation of several corrections to  $dE/dx$  in order to take into account the deviations from the Bethe theory at low and high energies as well as the effect of a finite nuclear size at ultra-relativistic energies. Special attention is paid to the transition energy region where the onset of the effect of a finite nuclear size is observed. Comparisons with experimental data and NIST data are presented.

*Key Words:* Heavy ions, ionization loss, MARS15 code

### 1 INTRODUCTION

The MARS code [1] is developed for detailed Monte Carlo modeling of hadronic and electromagnetic cascades in realistic geometry for various accelerator, shielding, detector and space applications. The recent needs of the Rare Isotope Accelerator, Relativistic Heavy-Ion Collider, Large Hadron Collider, and NASA projects was a stimulus to implement heavy-ion collision and transport physics into the MARS15 code [2]. The present paper describes in detail the ionization energy loss formalism employed in the code along with comparisons to experimental data and some recommended data. Radiative energy loss of heavy ions—bremsstrahlung and  $e^+e^-$  pair production—is described elsewhere. The ionization loss is of importance for correct prediction of radiation-induced effects, *e.g.* single-event upsets, in microelectronic devices. The lower energy limit in our stopping power model is equal to 1 keV per nucleon.

### 2 FORMALISM OF IONIZATION LOSS THEORY

In our model we distinguish three energy regions. Below 1 MeV per nucleon and above 10 MeV per nucleon the tabulated data on proton total stopping power from Ref. [3] and the Bethe formalism, respectively, are used in combination with all the corrections described below. Between the two energies, a *mix-and-match* procedure is used to perform an interpolation between the approaches. It should also be noted that the 10-MeV limit is identical to the one used when considering the ion effective charge (see below) and should be adjusted for some target nuclei to get better appearance of the ionization loss distributions.

---

\*Corresponding author

## 2.1 Bethe Theory

The mean ionization energy loss of charged particles heavier than electrons is given by the Bethe expression [4]

$$-\frac{1}{\rho} \frac{dE}{dx} = 4\pi N_A r_e^2 m_e c^2 z^2 \frac{Z}{A} \frac{1}{\beta^2} L(\beta) \quad (1)$$

where  $A$  and  $Z$  are the target atomic mass and number, respectively, and the other variables have their usual meaning. The ionization logarithm,  $L(\beta)$ , is presented in the following form:

$$L(\beta) = L_0(\beta) + \sum_i \Delta L_i \quad (2)$$

$$L_0(\beta) = \ln \left( \frac{2m_e c^2 \beta^2 \gamma^2}{I} \right) - \beta^2 - \frac{\delta}{2} \quad (3)$$

where  $I$  and  $\delta$  are the mean excitation energy and density correction, respectively. When neglecting all the corrections  $\Delta L_i$  and dealing only with the  $L_0(\beta)$ , the expression (1) is referred to as the Bethe equation. The corrections  $\Delta L_i$  described below are to take into account the deviations from the Bethe theory for ions at both low and high energies.

## 2.2 Lindhard-Sørensen Correction

Lindhard and Sørensen derived a relativistic expression for electronic stopping power of heavy ions taking into account a finite nuclear size [5]. They used the exact solution to the Dirac equation with spherically symmetric potential which describes scattering of a free electron by an ion. Thus, their expression,  $\Delta L_{LS}$ , provides for the corrections of order higher than  $z^2$  to ionization loss of heavy ions in both low and high energy regimes. At high energies the Lindhard-Sørensen ( $LS$ ) correction replaces the previously developed Mott correction and relativistic Bloch-Ahlen one, while at low energies  $\Delta L_{LS}$  reduces to the Bloch non-relativistic correction [6].

At moderately relativistic energies (see below) the following expression derived for point-like ions is valid:

$$\begin{aligned} \Delta L_{LS} = & \sum_{k=1}^{\infty} \left[ \frac{k}{\eta^2} \frac{k-1}{2k-1} \sin^2(\delta_k - \delta_{k-1}) \right. \\ & + \frac{k}{\eta^2} \frac{k+1}{2k+1} \sin^2(\delta_{-k} - \delta_{-k-1}) \\ & \left. + \frac{k}{4k^2-1} \frac{1}{\gamma^2 k^2 + \eta^2} - \frac{1}{k} \right] + \frac{\beta^2}{2} \end{aligned} \quad (4)$$

where  $\eta = \alpha z / \beta$ ,  $\delta_k$  is a relativistic Coulomb phase shift expressed with the argument of the complex Gamma function (for details see Ref. [6]), and  $k$  is a parameter used in the summation over partial waves. At higher energies, when  $\gamma m_e c R \simeq \hbar/2$  where  $R$  is the ion radius, a modification to the Coulomb phase shifts due to a finite nuclear size is not negligible and the expression for  $\Delta L_{LS}$  gets more complicated from computational standpoint. At ultra-relativistic energies, when  $\gamma m_e c R \gg \hbar/2$ , an asymptotic expression for  $L(\beta)$  is valid.

$$L_{ultra} = L_0(\beta) + \Delta L_{LS} = \ln \left( \frac{2c}{R\omega_p} \right) - 0.2 \quad (5)$$

where  $\omega_p$  is the plasma frequency,  $\sqrt{4\pi n e^2 / m_e}$ , and  $n$  is the average density of target electrons. The value of  $L_{ultra}$  reveals a weak dependence on target and projectile parameters.

In our model the expressions (4) and (5), valid for moderately relativistic and ultra-relativistic energies, respectively, are employed. In the intermediate energy region we interpolate between the two approaches using a *mix-and-match* procedure.

## 2.3 Low-Energy Corrections

### 2.3.1 Barkas correction

The Barkas effect, associated with a  $z^3$  correction to the stopping power, is well pronounced at low energies. For example, for a 2-MeV proton in gold the effect is responsible for about 8% of ionization energy loss [7]. The correction is due to target polarization effects for low-energy distant collisions and can be accounted for by the following expression:

$$L_0(\beta) + \delta/2 \rightarrow (L_0(\beta) + \delta/2) \left( 1 + 2 \frac{z}{\sqrt{Z}} F(V) \right) \quad (6)$$

where  $V = \beta\gamma/\alpha\sqrt{Z}$ . The function  $F(V)$  is a ratio of two integrals within a Thomas-Fermi model of the atom. In our model we follow the tabulations for the function from Refs. [6, 8].

### 2.3.2 Shell corrections

The original Bethe theory is valid when the velocity of the projectile is much higher than that of electrons in target atoms. Shell corrections should be taken into account at lower projectile velocities. The total shell correction can be presented in the following form [7, 9]:

$$\Delta L_{shell} = -\frac{C}{Z} \quad (7)$$

where  $C$  is equal to  $C_K + C_L + \dots$  and thus takes into account the contributions from different atomic shells. For  $C_K$  and  $C_L$  we follow the asymptotic expressions and tabulations from Refs. [10, 12] and [11, 12], respectively, derived with hydrogen-like wave functions. For all the other atomic shells, up to a combined  $O-P$  shell, the scaling procedures developed by Bichsel [9] are employed. It is assumed in the scaling that the corrections for the outer shells have the dependence on the projectile velocity similar to that of the outermost shell studied with exact calculations, *i.e.*  $L$  shell in our case.

### 2.3.3 Projectile effective charge

At low projectile velocities, the effect of electron capture and loss due to interactions with target atoms should be taken into account as well. At present, the projectile charge distributions that cover a more or less noticeable range of ions, targets, and velocities are not available. Therefore one can deal with various empirical and semi-empirical fitting expressions for the average or, in other words, effective charge,  $z_{eff}$ . The effective charge is to replace the bare projectile charge in all the relevant expressions.

For protons and other singly charged particles the effective charge is assumed to be equal to the bare charge down to the lower energy limit of the model, 100 keV/A. For  $\alpha$ -particles a special fit by Ziegler *et al.* [13] independent of target material is used at all particle energies,  $E$ .

$$z_{eff}/2 = 1 - \exp \left[ - \sum_{i=0}^5 a_i \ln^i(E) \right] \quad (8)$$

where  $E$  is in keV per nucleon and the coefficients  $a_0$  through  $a_5$  are equal to 0.2865, 0.1266,  $-0.001429$ , 0.02402,  $-0.01135$ , and 0.00175, respectively.

For all the other ions more elaborate fitting expressions that include a dependence on target material are used:

- A combination of the expressions (3.38) and (3.39) from Ref. [13] below 1 MeV/A;
- The procedure by Hubert *et al.* [14] above 10 MeV/A;
- An energy weighted average between the two energies.

For some target nuclei, however, it is necessary to adjust the upper energy limit to get the stopping power curves with better, without sharp transitions, appearance.

Calculated ratios of ion effective charge to bare charge are presented in Fig. 1. The effect of neutralization of the bare projectile charge with captured electrons increases with the target atomic number, being almost negligible for  $\alpha$ -particles at energies above a few keV per nucleon.

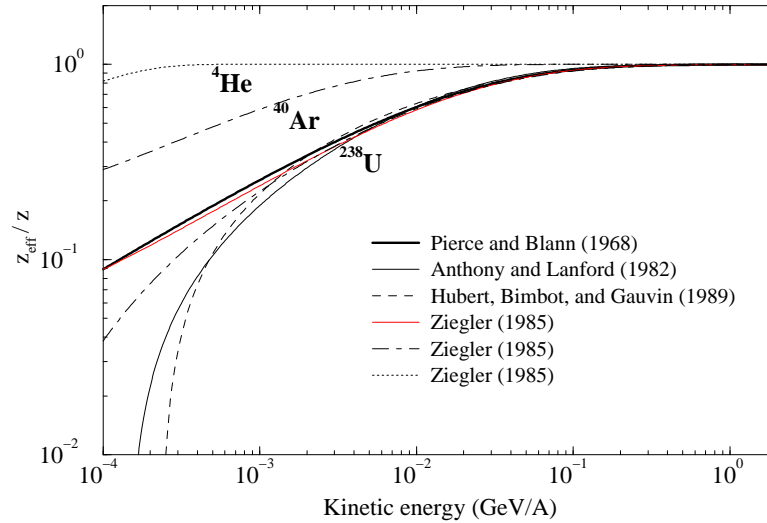


**Figure 1: Calculated effective charge of light and heavy ions,  $z_{eff}$ , in aluminum target relative to ion unscreened charge,  $z$ .**

### 3 VERIFICATION

#### 3.1 Comparison to experimental data

Here we compare calculated ionization loss to experimental data for several light and heavy ions. For  $\alpha$ -particles at low energies the overall agreement is very good (see Fig. 2). The

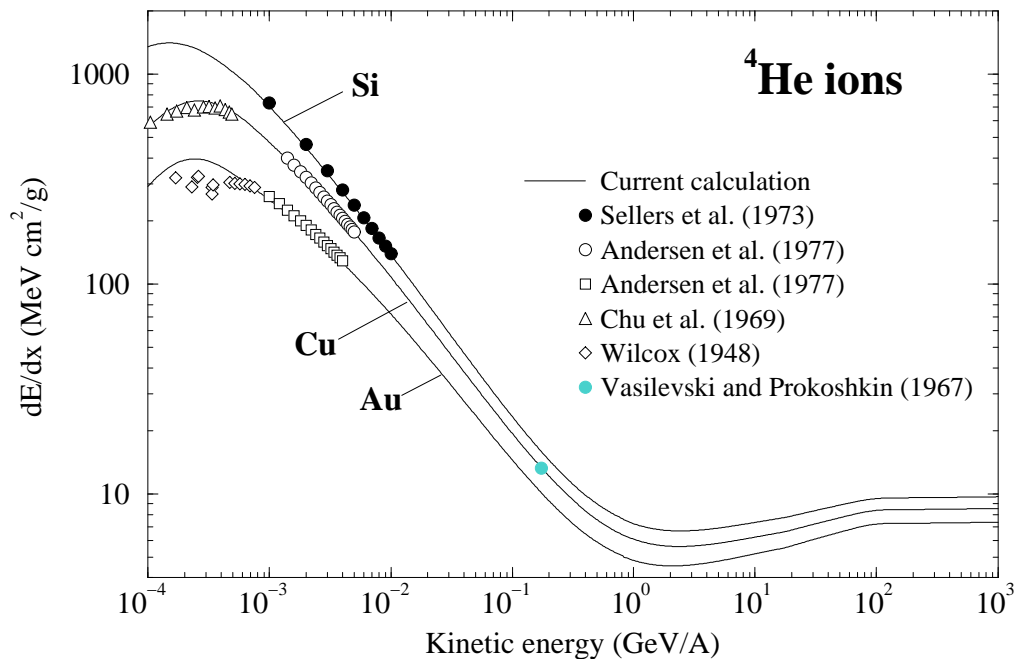


**Figure 2: Calculated ionization loss of  $\alpha$ -particles in various targets vs. experimental data [15].**

deviations from the Bethe theory due to the above-mentioned corrections, except for the shell corrections, increase with projectile charge,  $z$ , at both low and high energies. Therefore, the comparisons for super-heavy ions are interesting and important most of all.

At relativistic energies a comparison to experimental data is presented in Fig. 3 for a dozen of projectile-target combinations. One can make the following conclusions from the Figure: (i) the  $LS$  correction in this case provides for an agreement with experimental data within 2%; (ii) the above-mentioned combination of relativistic Bloch, Mott, and Ahlen (BMA) corrections gives rise to a systematic underestimation of ionization loss (2-3% for Xe ions) when compared to the  $LS$  approach; (iii) the difference between the BMA and  $LS$  approaches increases with projectile charge. This confirms that the Lindhard-Sørensen theory is correctly chosen.

A comparison to experimental data for super-heavy ions of lead and uranium is given in Fig. 4. One can see that the employed *mix-and-match* procedure provides for a good, within 10%, agreement with experiment at low energies. For uranium ions the density effect is well seen at

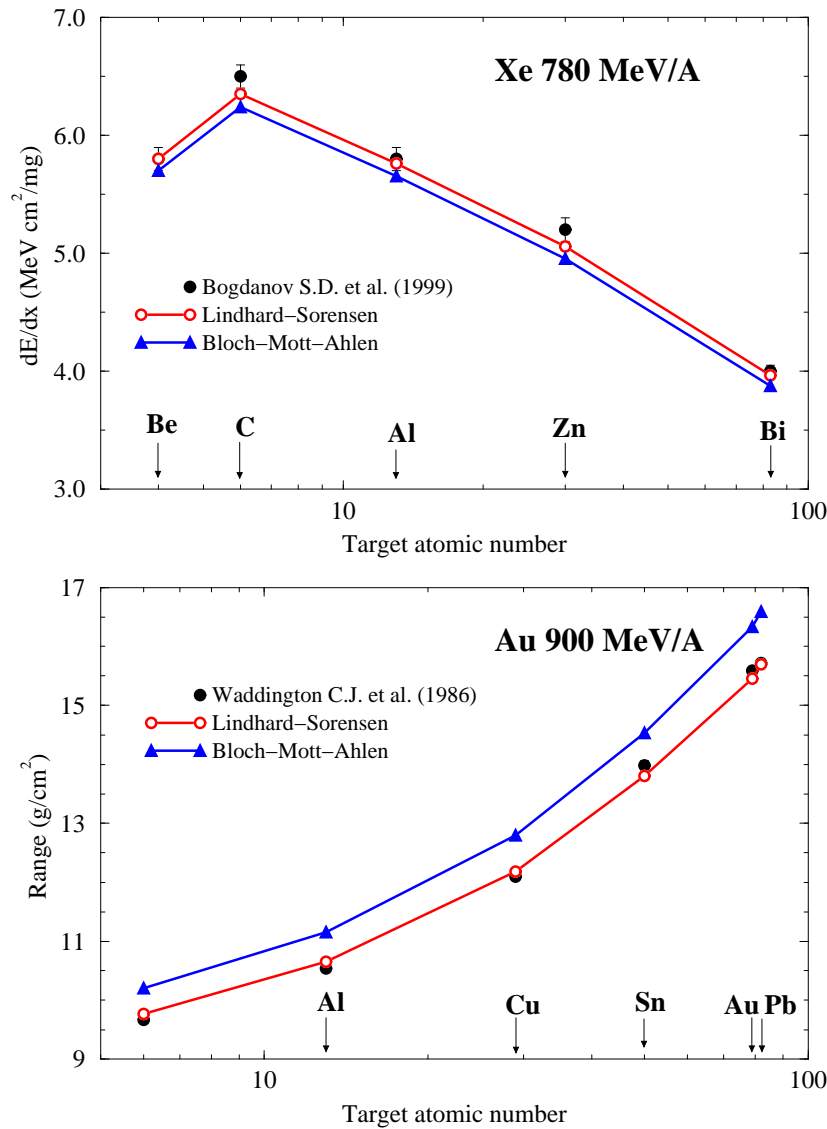


**Figure 3: Calculated (lines with symbols) ionization loss and range of relativistic heavy ions in various targets vs. experimental data (pure symbols) [16]. The corrections to the ionization logarithm,  $\Delta L$ , were calculated following the Lindhard- Sørensen and Bloch-Mott-Ahlen formalisms (see above).**

ultra-relativistic energies—the highest ionization loss is observed for the target of the lowest density, *i.e.* gaseous argon. For lead ions at ultra-relativistic energies the effect of finite nuclear size, that gives rise to a saturation of ionization loss instead of a logarithmic growth characteristic of a pointlike projectile, is easily recognized. The experimental data at 160 GeV/u by Datz *et al.* [17] corresponds to the highest energy achieved when accelerating heavy ions.

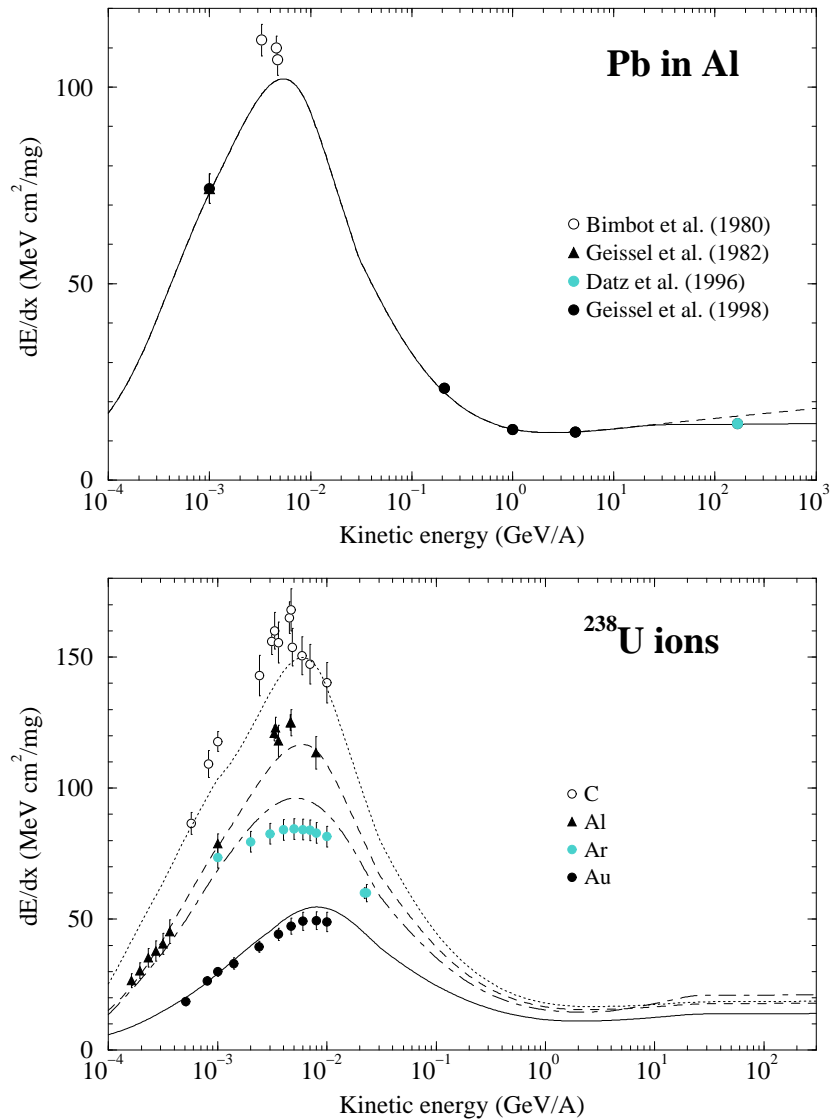


**Figure 4: Calculated (lines) ionization loss vs. experimental data (symbols) for lead ions in aluminum (top) and uranium ions in several targets (bottom) [17]. For lead ions the dashed line indicates calculation for pointlike projectiles.**

### 3.2 Comparison to NIST data

A comparison between the ionization loss calculated within the framework of the described formalism and the data by NIST [3] is presented in Fig. 5 for protons and  $\alpha$ -particles. The data of Ref. [3] are given up to 10<sup>4</sup> MeV and 250 MeV/A for protons and  $\alpha$ -particles, respectively. One can see that the agreement between the MARS15 and NIST ionization loss is within 1.3% for protons in the entire energy region. The agreement is somewhat better than that of MCNP5 [18] where the difference is about 3% for the energy region from 4 up to 10<sup>4</sup> MeV, being more than

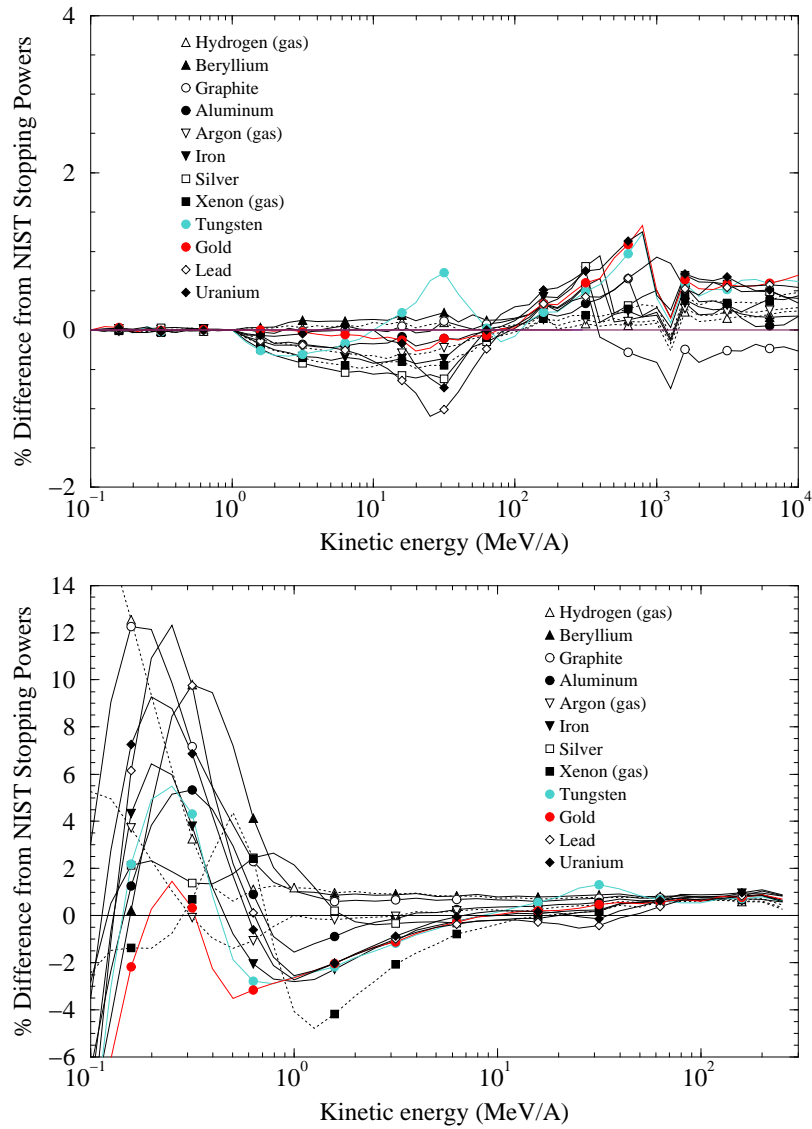


**Figure 5: A comparison of MARS15 proton (top) and  $\alpha$ -particle (bottom) ionization loss in several elements to NIST data.**

10% below 4 MeV.

For  $\alpha$ -particles the biggest difference, about 10-15%, is observed below 400 keV/A. The difference is comparable to the disagreement between theory and experiment in the energy region. As far as the tabulated proton data of Ref. [3] are used below 1 MeV/A in our model, the differences can be attributed to the description of effective charge of  $\alpha$ -particles. Above 10 MeV per nucleon the observed difference between the MARS15 and NIST ionization loss is about 1%. One can see that approximately a half of the 1% is due to the difference in the description of the proton ionization loss.

## 4 CONCLUSIONS

The various corrections to the Bethe mean ionization loss theory, as implemented in the MARS15 Monte Carlo code, are described. The comparisons of calculated ionization loss to the NIST published values reveal good overall agreement for protons and  $\alpha$ -particles. The agreement between the current model and experimental data is very good up to the super-heavy ions of lead and uranium.

Experimental programs at many accelerator facilities cover wide energy regions. For example, the Rare Isotope Accelerator is supposed to be operated at energies from a few keV/A up to hundreds of MeV/A. To meet such practical demands, the developments are underway to validate our model in the 1–100 keV/A region.

## 5 ACKNOWLEDGMENTS

This work was supported by the Universities Research Association, Inc., under contract DE-AC02-76CH03000 with the U.S. Department of Energy.

## 6 REFERENCES

1. N. V. Mokhov, "Status of MARS Code," *Proc. Workshop on Shielding Aspects of Accelerators, Targets and Irradiation Facilities (SATIF-6)*, SLAC, Menlo Park, CA, April 10-12, 2002, pp. 407-416 (2004).
2. N. V. Mokhov, K. K. Gudima, S. G. Mashnik, I. L. Rakhno, S. I. Striganov, "Towards a Heavy-Ion Transport Capability in the MARS15 Code," *Proc. 10<sup>th</sup> Int. Conf. on Radiation Shielding*, Funchal (Madeira), Portugal, May 9-14, 2004; Fermilab-Conf-04/052-AD (2004).
3. "Physical Reference Data," National Institute of Standards and Technology, <http://physics.nist.gov/PhysRefData/Star/Text/contents.html> (2000).
4. H. Bichsel, D. E. Groom, and S. R. Klein, "Passage of Particles through Matter," *Phys. Rev.*, **D66**, p. 010001-195 (2002).
5. J. Lindhard and A. Sørensen, "Relativistic theory of stopping for heavy ions," *Phys. Rev.*, **A53**, pp. 2443-2456 (1996).
6. B. A. Weaver, A. J. Westphal, "Energy loss of relativistic heavy ions in matter," *Nucl. Instrum. Meth. Phys. Res.*, **B187**, pp. 285-301 (2002).
7. *Stopping Powers for Electrons and Positrons. ICRU Report 37*, International Commission on Radiation Units and Measurements, Bethesda, USA (1984).
8. J. D. Jackson, R. L. McCarthy, " $z^3$  corrections to energy loss and range," *Phys. Rev.*, **B6**, pp. 4131-4141 (1972).
9. *Stopping Powers and Ranges for Protons and Alpha Particles. ICRU Report 49*, International Commission on Radiation Units and Measurements, Bethesda, USA (1993).
10. M. C. Walske, "The Stopping Power of K-Electrons," *Phys. Rev.*, **88**, pp. 1283-1289 (1952).
11. M. C. Walske, "Stopping Power of L-Electrons," *Phys. Rev.*, **101**, pp. 940-944 (1956).

12. G. S. Khandelwal, "Shell Corrections for K- and L-Electrons," *Nucl. Phys.*, **A116**, pp. 97-111 (1968).
13. J. F. Ziegler, J. P. Biersack, U. Littmark, *The Stopping and Range of Ions in Solids. Vol. 1*, Pergamon Press, Oxford, England (1985).
14. F. Hubert, R. Bimbot and H. Gauvin, "Semi-Empirical Formulae for Heavy Ion Stopping Powers in Solids in the Intermediate Energy Range," *Nucl. Instrum. Meth. Phys. Res.*, **B36**, pp. 357-363 (1989).
15. H. H. Andersen, J. F. Bak, H. Knudsen, and B. R. Nielsen, "Stopping Power of Al, Cu, Ag, and Au for MeV hydrogen, helium, and lithium ions.  $Z_1^3$  and  $Z_1^4$  proportional deviations from the Bethe formula," *Phys. Rev.*, **A16**, pp. 1929-1940 (1977); B. Sellers, A. Hanser, J. G. Kelley, "Energy Loss and Stopping Power measurements between 2 and 10 MeV/amu for  $^3\text{He}$  and  $^4\text{He}$  in Silicon," *Phys. Rev.*, **B8**, pp. 98-102 (1973); H. A. Wilcox, "Experimental Determination of Rate of Energy Loss for Slow  $\text{H}^1$ ,  $\text{H}^2$ ,  $\text{He}^4$ ,  $\text{Li}^6$  Nuclei in Au and Al," *Phys. Rev.*, **74**, pp. 1743-1754 (1948); W. K. Chu and D. Powers, "Alpha-Particle Stopping Cross Section in Solids from 400 keV to 2 MeV," *Phys. Rev.*, **187**, pp. 478-490 (1969); I. M. Vasilevski and Yu. D. Prokoshkin, "Ionization Energy Loss of Protons, Deuterons, and  $\alpha$  Particles," *Sov. J. Nucl. Phys.*, **4**, pp. 390-494 (1967).
16. S. D. Bogdanov, S. S. Bogdanov, E. E. Zhurkin, and V. F. Kosmach, "Investigation of the Passage of 10 – 1000-MeV/nucleon superheavy ions through homogeneous media," *J. of Experim. and Theor. Phys.*, **88**, pp. 220-226 (1999); C. J. Waddington, D. J. Fixseen, H. J. Crawford *et al.*, "Stopping of Relativistic Heavy Ions in Various Media," *Phys. Rev.*, **A34**, pp. 3700-3711 (1986).
17. R. Bimbot, D. Gardes, H. Geissel, *et al.*, "Stopping Power Measurements for 3 – 5-MeV/nucleon  $^{86}\text{Kr}$ ,  $^{132}\text{Xe}$ ,  $^{208}\text{Pb}$  and  $^{238}\text{U}$  in Solids," *Nucl. Instrum. Meth.*, **174**, pp. 231-236 (1980); H. Geissel, Y. Laichter, W. F. W. Schneider, *et al.*, "Energy Loss and Energy Loss Straggling of Fast Heavy Ions in Matter" *Nucl. Instrum. Meth.*, **194**, pp. 21-29 (1982); S. Datz, H. F. Krause, C. R. Vane, *et al.*, "Effect of Nuclear Size on the Stopping Power of Ultrarelativistic Heavy Ions," *Phys. Rev. Lett.*, **77**, pp. 2925-2928 (1996); H. Geissel, C. Scheidenberger, "Slowing Down of Relativistic Heavy Ions and New Applications," *Nucl. Instrum. Meth. Phys. Res.*, **B136-138**, pp. 114-124 (1998); H. Geissel, H. Weick, C. Scheidenberger, *et al.*, "Experimental Studies of Heavy-Ion Slowing Down in Matter," *Nucl. Instrum. Meth. Phys. Res.*, **B195**, pp. 3-54 (2002); M. D. Brown and C. D. Moak, "Stopping Power of Some Solids for 30 – 90-MeV  $^{238}\text{U}$  Ions," *Phys. Rev.*, **B6**, pp. 90-94 (1972); R. Bimbot, S. Barbey, T. Benfoughal, *et al.*, "Stopping Power of Gases for Heavy Ions," *Nucl. Instrum. Meth. Phys. Res.*, **B107**, pp. 9-14 (1996).
18. T. Goorley, R. E. Prael, H. G. Hughes, "Verification of Stopping Powers for Proton Transport in MCNP5," *Proc. American Nucl. Soc. Winter Mtg.*, New Orleans, Louisiana, USA, Nov. 16-20, 2003.